Structural and optical studies of high dielectric constant $(Na_{0.5}A_{0.5})Cu_3Ti_4O_{12}$ (A = La and Bi)

2008 J. Phys.: Condens. Matter 20 275238

(http://iopscience.iop.org/0953-8984/20/27/275238)

J. Phys.: Condens. Matter **20** (2008) 275238 (8pp) doi:10.1088/0953-8984/20/27/275238

Structural and optical studies of high dielectric constant $(Na_{0.5}A_{0.5})Cu_3Ti_4O_{12}$ (A = La and Bi)

K-C Liang[1], H L Liu[1,5], H D Yang[2], W N Mei[3] and D C Ling[4]

[1] Department of Physics, National Taiwan Normal University, Taipei 116, Taiwan
[2] Department of Physics, National Sun Yat-Sen University, Kaoshiung 804, Taiwan
[3] Department of Physics, University of Nebraska at Omaha, Omaha, NE 68182-0266, USA
[4] Department of Physics, Tamkang University, Tamsui 251, Taiwan

Received 8 February 2008, in final form 13 May 2008
Published 13 June 2008
Online at stacks.iop.org/JPhysCM/20/275238

Abstract

We report x-ray powder diffraction and temperature-dependent infrared reflectivity measurements of $(Na_{0.5}La_{0.5})Cu_3Ti_4O_{12}$ and $(Na_{0.5}Bi_{0.5})Cu_3Ti_4O_{12}$ in order to investigate the origin of their lower room-temperature dielectric constants in comparison with the giant value of $CaCu_3Ti_4O_{12}$. Substituting Ca with Na/La or Na/Bi is found to decrease all Ti–O–Ti angles by the TiO_6 octahedra tilts, resulting in an increase of the local structural disorder on the Na/La and Na/Bi compounds. Further, several infrared-active phonon modes show a broadening in their linewidths, reflecting that the coherency in these vibrational modes is degraded by disorder. Additionally, the lowest-frequency mode of the Ca material is observed to strengthen dramatically at low temperatures, but to a lesser extent in the Na/La and Na/Bi compounds. These results suggest the important role of the local structural disorder on the anomalous low-frequency dielectric response in these materials.

(Some figures in this article are in colour only in the electronic version)

1. Introduction

The complex perovskite oxides $ACu_3Ti_4O_{12}$ have recently attracted enormous attention, stimulated not only by the potential technological usefulness of their high dielectric constant but also by the need to understand the mechanism underlying their unusual dielectric response [1, 2]. Among them, $CaCu_3Ti_4O_{12}$ (CCTO) [3, 4] possesses the largest low-frequency dielectric constant ($\epsilon_1 \sim 10^5$) over a broad temperature range extending from 100 to 600 K. Moreover, above a critical frequency that ranges between 10 Hz and 1 MHz depending on temperature, its ϵ_1 drops to a value of about 100, typical of conventional perovskite insulators. Usually, a large dielectric constant results from atomic displacements in a non-centrosymmetrical structure near its phase transition temperature, e.g. in an ferroelectric. However, CCTO has a body-centered cubic perovskite-related structure and there are no anomalies in crystal structure and lattice vibrations down to 35 K [5, 6]. It has been suggested that the large dielectric constant of CCTO is unlikely to originate from its intrinsic property [7, 8] but from microstructures of the ceramic sample or single crystal. Indeed, a number of recent experiments [9–12] have shown that the high dielectric constant of CCTO could be due to the creation of internal barrier layer capacitances (IBLC), presumably at twin boundaries, or at the interfaces between grains and grain boundaries, or between sample and electrodes.

Because vibrational spectroscopy can provide unique information about materials, including phonon modes, the presence of impurities or defects, ordering and the orientation of dipoles, infrared spectral studies of these materials are of great interest. Infrared measurements on the CCTO and $CdCu_3Ti_4O_{12}$ compounds were first reported by Homes *et al* [4, 6]. The low-frequency vibrational modes ($\omega < 300\ cm^{-1}$) of CCTO are observed to strengthen dramatically at low temperatures, indicating that the Born effective charges are increasing in the unit cell. At far-infrared frequencies, the value of the dielectric constant of CCTO is about 60, which is far smaller than the value of about 10^5 obtained at lower radio-frequencies. This suggests that the extrinsic effects are

[5] Author to whom any correspondence should be addressed.

likely sources of the unusual low-frequency dielectric behavior of CCTO. Homes *et al* [4, 6] proposed that the IBLC effect results in a giant dielectric constant of CCTO and that the rapid reduction of dielectric constant at low temperature is due to the removal of an IBLC mechanism. Recently, Kant *et al* [13] compared the results of far- and mid-infrared measurements with those obtained by broadband dielectric and millimeter-wave spectroscopy on the same CCTO single crystal. They found that the static dielectric constant derived from the far-infrared experiments nicely scales with that measured by 1 GHz spectroscopy; in particular, they show a similar temperature dependence. In addition, the strong increase of dielectric constant as detected at lower frequencies corresponds to Maxwell–Wagner-like effects [10, 14, 15]. However, to date, only the spectra of CCTO and $CdCu_3Ti_4O_{12}$ (CdCTO) have been reported despite the large number of $ACu_3Ti_4O_{12}$ compounds studied [2], more than ten of them having dielectric constants larger than 1000 at room temperature.

In this paper, we present the x-ray powder diffraction and temperature-dependent infrared reflectivity measurements of $Na_{0.5}La_{0.5}Cu_3Ti_4O_{12}$ (NLCTO) and $Na_{0.5}Bi_{0.5}Cu_3Ti_4O_{12}$ (NBCTO). The results are compared with those of CCTO. The dielectric constants of NLCTO and NBCTO were reported to be 3560 and 2454 at 25 °C and 10^5 Hz [2]. At room temperature, x-ray-diffraction data show that all Ti–O–Ti angles decrease from a value of 144° for CCTO to 134° for NBCTO by the TiO_6 octahedra tilts, indicating the replacement of Ca with Na/La or Na/Bi ions causes significant changes in the environment surrounding the TiO_6 octahedra. Moreover, several infrared-active phonon peaks show a broadening in their linewidths for the NLCTO and NBCTO samples, reflecting that the coherency of these vibrational modes is degraded by disorder. With decreasing temperature, the lowest-frequency phonon mode shifts to lower energies and exhibits increased linewidths and spectral weights. Similar behaviors have also been observed in CCTO [4, 6, 13], but to a lesser extent in NLCTO and NBCTO. These data suggest that the local structural disorder has an important connection with the anomalous low-frequency dielectric response for these materials.

2. Experiment

Disc-shaped polycrystalline samples with a diameter of 5 mm and thickness of 2 mm were prepared by conventional solid-state powder processing techniques. A detailed description of the process can be found elsewhere [11]. Figure 1 shows the temperature dependence of the molar magnetic susceptibility of NLCTO and NBCTO in a zero-field-cooled run with a magnetic field of 1000 G, clearly revealing that they have an antiferromagnetic phase transition. The Néel temperature for NLCTO and NBCTO is about 24 K and 27 K, respectively. The structure and phase purity of the samples were checked by x-ray powder diffraction. Data were analyzed using the GSAS program [16]. For refinements at all samples the space group $Im3$ was used.

The samples were polished with 0.05 μm grain size Al_2O_3 powders until an optically reflecting surface was achieved.

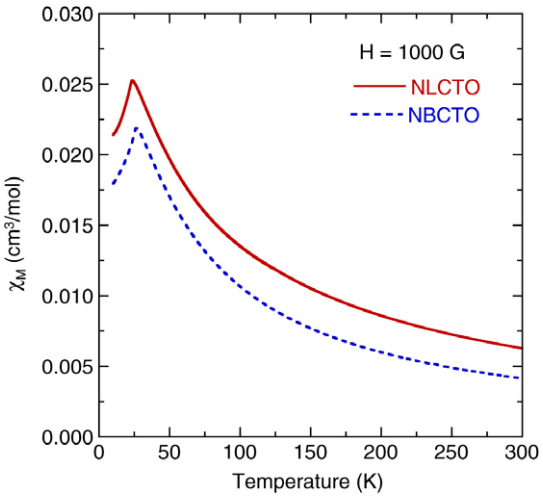

Figure 1. Zero-field-cooled magnetic susceptibility as a function of temperature for NLCTO and NBCTO with a magnetic field of 1000 G.

Near-normal infrared and optical reflectance measurements were then carried out over a wide frequency range using two different spectrometers. A Bruker IFS 66v Fourier transform infrared spectrometer was used in the far-infrared and mid-infrared regions (30–6000 cm^{-1}), while the near-infrared to near-ultraviolet regions (4000–55000 cm^{-1}) were covered using a Perkin-Elmer Lambda-900 spectrometer. The modulated light beam from the spectrometer was focused onto either the sample or an Au (Al) reference mirror, and the reflected beam was directed onto a detector appropriate for the frequency range studied. The different sources and detectors used in these studies provided substantial spectral overlap, and the reflectance mismatch between adjacent spectral ranges was less than 1%. For low-temperature measurements, the sample was mounted in a continuous-flow helium cryostat equipped with a thermometer and heater near the cryostat tip, regulated by a temperature controller.

The optical properties (i.e. the complex conductivity $\sigma(\omega) = \sigma_1(\omega) + i\sigma_2(\omega)$ or dielectric constant $\epsilon(\omega) = 1 + 4\pi i\sigma(\omega)/\omega$) were calculated from a Kramers–Kronig analysis of the reflectance data [17]. Because a large frequency region was covered, a Kramers–Kronig analysis should provide reasonably accurate values of the optical constants[6]. To perform these transformations one needs to extrapolate the reflectance at both low and high frequencies. At low frequencies the extension was done by modeling the reflectance using the Lorentz model and using the fitted results to extend the reflectance below the lowest frequency measured in the experiment. The high-frequency extrapolations were done by using a weak power law dependence, $R \approx \omega^{-s}$ with $s \approx 1$–2.

[6] We notice that a polycrystalline sample is an inhomogeneous medium whose physical properties vary spatially due to crystal-to-crystal orientation. In our samples, a local response can be justified because the grain size (diameter ~0.1 μm after polishing) is much smaller than the wavelength of the light in the range of interest. Additionally, since CCTO, NLCTO and NBCTO have a nearly three-dimensional structure, their optical constants should be nearly isotropic. The Lorentzian fitting analysis could be applied to our polycrystalline samples without much problem.

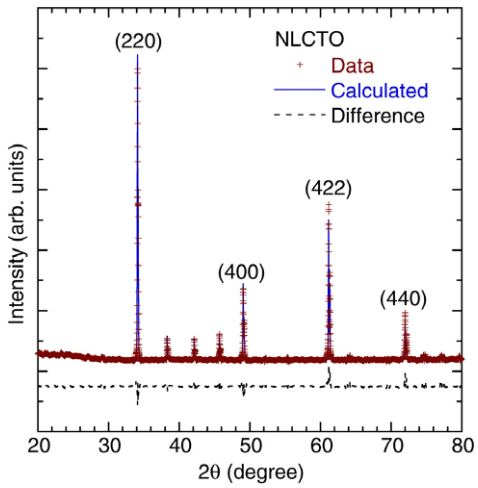

Figure 2. Observed, calculated and difference x-ray powder diffraction patterns for NLCTO.

Table 1. Crystallographic data for CCTO, NLCTO and NBCTO.

	CCTO	NLCTO	NBCTO
x (O)	0.302 901(1)	0.294 162(1)	0.317 3(9)
y (O)	0.189 572(1)	0.173 155(1)	0.166 9(10)
A–O (Å)	2.640 70(1)	2.528 04(1)	2.657(9)
Cu–O (Å)	2.020 95(1)	1.992 14(1)	1.834(4)
Ti–O (Å)	1.940 50(1)	1.964 46(1)	2.0155(18)
O–Ti–O (deg)	88.907(1)	93.893(1)	88.73(35)
O–Ti–O (deg)	91.093(1)	86.107(1)	91.27(35)
O–Cu–O (deg)	87.770(1)	80.142(1)	84.8(6)
O–Cu–O (deg)	92.230(1)	99.858(1)	95.2(6)
Ti–O–Ti (deg)	144.381(1)	140.959(1)	133.67(24)
a (Å)	7.390 04	7.406 18	7.412 00
R_p (%)	4.58	4.39	7.15
R_{wp} (%)	6.39	6.25	9.67

3. Results and discussion

3.1. X-ray diffraction

Figure 2 shows the diffraction profile, the Rietveld refinement and the difference pattern for NLCTO at room temperature. All the reflections can be indexed and no impurity phases are apparent above the background level. From the Rietveld refinement we determined the lattice constants of the samples under investigation. The crystallographic data of CCTO, NLCTO and NBCTO are listed in table 1. Two interesting structural properties have been revealed by the fitting results. First, the lattice parameter of CCTO is $a = 7.390\,04$ Å, in good agreement with those reported by Subramanian *et al* [1]. The NLCTO and NBCTO have larger lattice constants (7.406 18 Å and 7.412 00 Å, respectively). Second, the structure of $ACu_3Ti_4O_{12}$ is best viewed as a network of corner-shared TiO_6 octahedra where all Ti–O–Ti angles are 180° in the ideal structure. Most of the distortions of the perovskite structure are based on tilting of the TiO_6 octahedra, where some or all of the Ti–O–Ti angles are bent away from 180°. Notably, the Ti–O–Ti angles of CCTO, NLCTO and NBCTO are reduced to about 144°, 141° and 134°, resulting in an increase of the octahedral tilts.

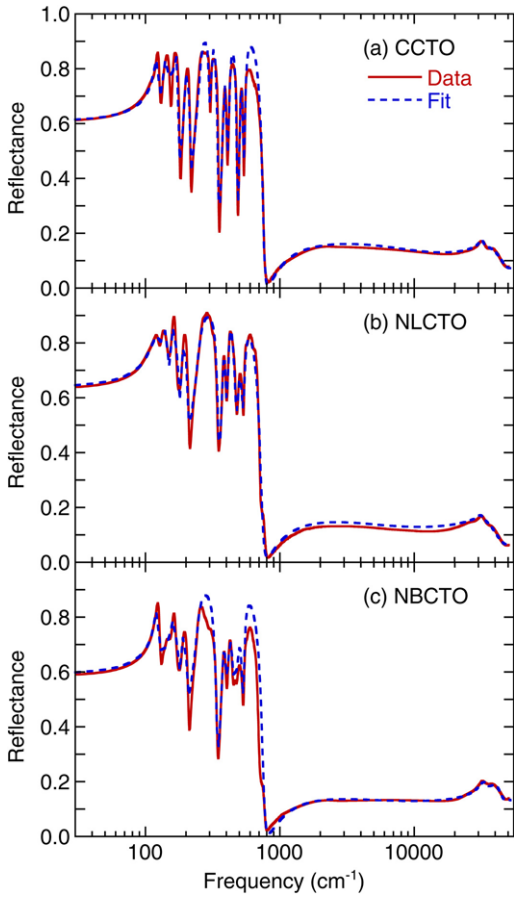

Figure 3. Room-temperature optical reflectance spectra (solid lines) of the (a) CCTO, (b) NLCTO and (c) NBCTO compounds. The dashed lines are the best fit using the Lorentzian model.

3.2. Reflectance measurements

The measured room-temperature optical reflectance spectra of CCTO, NLCTO and NBCTO are shown in figure 3. In all cases, the spectra of the samples reveal the characteristic of an insulator at low frequencies. A number of phonon features are observed in the far-infrared region. For higher frequencies, the spectra are almost dispersionless, showing only several weak electronic features. The reflectance is modeled using Lorentzian oscillators:

$$\epsilon(\omega) = \sum_{j=1}^{N} \frac{\omega_{pj}^2}{\omega_j^2 - \omega^2 - i\omega\gamma_j} + \epsilon_\infty, \qquad (1)$$

where ω_j, γ_j and ω_{pj} are the frequency, damping and oscillator strength of the jth Lorentzian contribution; and ϵ_∞ is the high-frequency limit of $\epsilon(\omega)$ which includes interband transitions at frequencies above the measured range. The parameters used to fit the measured optical data are listed in table 2. The spectra are well reproduced by considering 10, 9 and 10 Lorentzian oscillators representing the phonon peaks of CCTO, NLCTO and NBCTO, respectively, and 4 for the electronic interband transitions of the three samples. Figure 4 shows the frequency-dependent optical conductivity $\sigma_1(\omega)$ of the CCTO, NLCTO and NBCTO compounds. The spectra of all

Table 2. Parameters of a Lorentzian fit for the room-temperature optical reflectance data.

Mode	CCTO			NLCTO			NBCTO		
	ω_j (cm^{-1})	γ_j (cm^{-1})	ω_{pj} (cm^{-1})	ω_j (cm^{-1})	γ_j (cm^{-1})	ω_{pj} (cm^{-1})	ω_j (cm^{-1})	γ_j (cm^{-1})	ω_{pj} (cm^{-1})
1	121	6.9	515	118	14.6	654	121	6.8	467
2	140	9.3	527	134	12.9	522	147	20.8	469
3	161	7.1	383	157	9.4	415	159	12.8	404
4	199	8.9	432	189	10.4	394	189	14.2	399
5	257	15.9	850	252	27.3	959	247	25.7	901
6	308	10	305						
7	382	14.5	522	374	19.9	491	376	20.8	498
8	422	17.7	558	411	17.8	403	414	33.9	489
9							458	27	248
10	504	15.9	435	488	41.3	396	485	44	437
11	551	19.8	470	541	35.4	359	543	27	386
	20203	71389	29168	20128	127290	26895	20871	143544	22292
	31918	3213	8985	31375	3548	7707	33450	5012	15381
	38144	23941	45809	34965	22551	44126	40607	13530	41092
	58584	10704	26185	56575	13771	24800	51831	11036	30076
	$\epsilon_\infty =$	2.18			2.32			2.76	

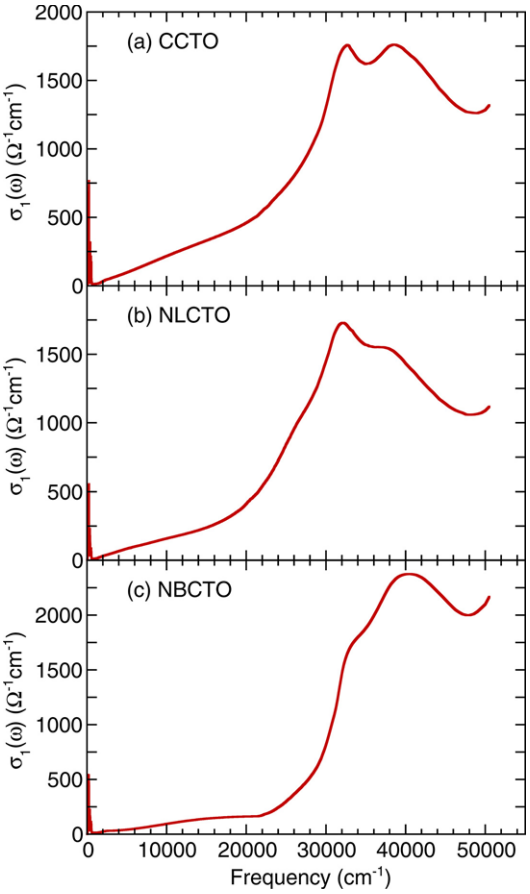

Figure 4. Real part of room-temperature optical conductivity spectra of the (a) CCTO, (b) NLCTO and (c) NBCTO compounds.

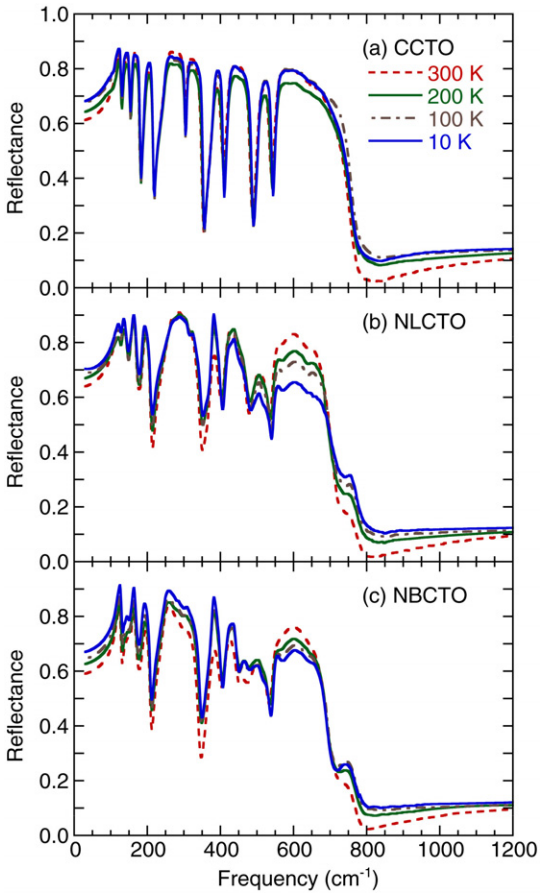

Figure 5. The temperature dependence of the infrared reflectance of the (a) CCTO, (b) NLCTO and (c) NBCTO compounds.

samples can be described in general terms as (i) sharp phonon resonances below 800 cm^{-1} and (ii) four absorption bands above 20 000 cm^{-1} that can be associated with charge-transfer transitions between O 2p and Ti 3d (t_{2g} or e_g) states [18]. The position and intensity of the phonon peaks and electronic bands are perturbed to some extent by doping, reflecting changes in the environments surrounding the TiO_6 octahedra.

The temperature-dependent infrared reflectance of CCTO, NLCTO and NBCTO between 30 and 1200 cm^{-1} are

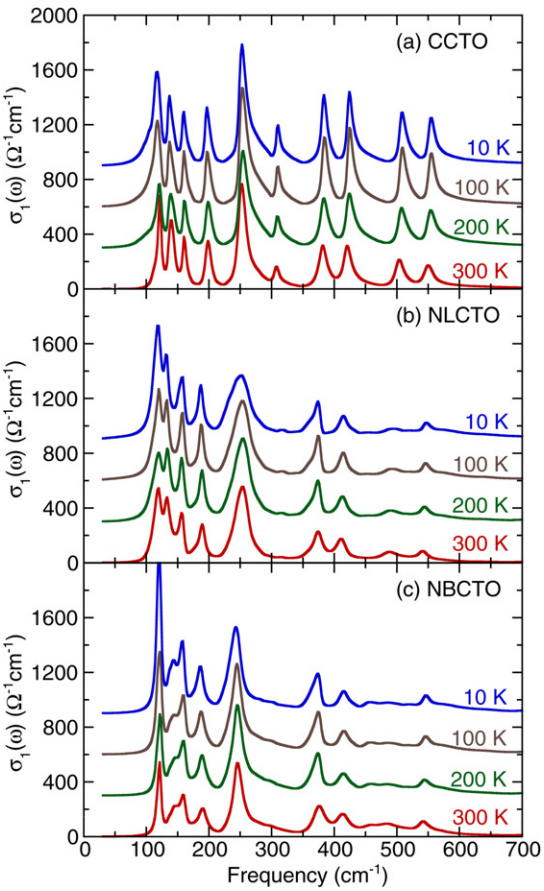

Figure 6. Far-infrared conductivity spectra of the (a) CCTO, (b) NLCTO and (c) NBCTO compounds. For clarity, the ordinate has been offset by 30% of the maximum of the Y axis for successive spectra.

presented in figure 5. The spectra do not change significantly with temperature, which implies that there is no structural phase transition within the temperature range investigated. Figure 6 shows the temperature dependence of the far-infrared conductivity. Consider first the room-temperature phonon response in figure 6. According to factor group analysis [7], CCTO has a cubic perovskite-like structure with space group $Im3$ in which a total of eleven infrared-active T_u modes are expected. The room-temperature $\sigma_1(\omega)$ of CCTO exhibits ten phonon resonances. These phonon eigenfrequencies are close to those reported for single crystals [6, 13]. The four low-frequency peaks at about 121, 140, 161 and 199 cm^{-1} correspond to the external mode of the Ca cation ions. Two vibrations observed at about 257 and 308 cm^{-1} are related to the Cu–O movements. The four phonon modes are seen at about 382, 422, 504 and 551 cm^{-1}, which are connected with the Ti–O vibrations. Notably, these modes show a shift of the peak position to lower frequencies by 3–16 cm^{-1} and a broadening of the resonance linewidth in the NLCTO and NBCTO compounds. The 308 cm^{-1} peak observed in CCTO is hardly detected in NLCTO due to its low oscillator strength. The infrared spectrum of NBCTO has one more feature at about 458 cm^{-1}, leading to the suggestion that this lattice mode is an indication of an additional structural complexity.

With decreasing temperature, there are several key features observed in the optical spectra shown in figure 6, including (i) the phonon peaks of three samples below 300 cm^{-1} shift to lower frequency and have some conspicuous area increase at lower temperature, whereas the ones above 300 cm^{-1} shift to higher frequency and become narrower; (ii) the lowest-frequency vibrational mode at about 121 cm^{-1} has a remarkable increase in linewidth and intensity with decreasing temperature; and (iii) the above-mentioned behavior becomes smaller with the replacement of Ca ions with Na/La or Na/Bi ions, except the phonon mode (257 cm^{-1} in CCTO, 252 cm^{-1} in NLCTO and 247 cm^{-1} in NBCTO) shifts to lower frequencies (255 cm^{-1} in CCTO, 249 cm^{-1} in NLCTO and 242 cm^{-1} in NBCTO). As prototypical examples, figures 7 and 8 illustrate the frequency, damping and oscillator strength of phonons 1 and 8 as a function of temperature. The hardening mode above 300 cm^{-1} can be explained by means of thermal effects. Anharmonic interactions are relevant to the high-order terms of the atomic vibrations beyond traditional harmonic terms. The temperature-dependent phonon frequency and linewidth can be written as [19]

$$\omega(T) = \omega_0 \left(1 - \frac{a}{\exp(\Theta/T) - 1}\right), \tag{2}$$

and

$$\gamma(T) = \gamma_0 \left(1 + \frac{b}{\exp(\Theta/T) - 1}\right), \tag{3}$$

where ω_0 and γ_0 are the harmonic frequency of the optical mode and the line broadening due to defects. a and b are the anharmonic coefficients. Θ is the Debye temperature, which can be estimated from an average of all infrared-active phonon frequencies. For the analysis of the anharmonic contributions, Debye temperatures of 438 K (CCTO), 426 K (NLCTO) and 452 K (NBCTO) have been determined. The solid lines in figure 8 are the theoretical predictions based on equations (2) and (3), which are in good agreement with the experimental data.

The anomalous increase in oscillator strength of the low-frequency modes of CCTO was previously observed by Homes [4, 6] and Kant *et al* [13]. More interestingly, the total oscillator strength summed over all infrared modes is also observed to rise, growing by ∼19% from 300 to 10 K in CCTO, ∼16% in NLCTO and ∼15% in NBCTO. This implies the redistribution of charges within the until cell with varied temperature. The oscillator strength ω_{pj} of each phonon mode can be used to estimate the Born effective charge on each ion. An expression based on a rigid-ion model of lattice dynamics has been applied successfully to other systems with ionic character [20]. The formula is

$$\frac{1}{\epsilon_\infty} \sum_j \omega_{pj}^2 = \frac{4\pi}{V_c} \sum_k \frac{(Z_k^* e)^2}{M_k}, \tag{4}$$

where $\sum_k Z_k^* = 0$, V_c is the unit cell volume, and j and k index the lattice modes and the atoms with mass M_k, respectively. In oxide materials, oxygen is often the lightest element, so that the summation is dropped and the change in the effective charge is associated purely with the oxygen (i.e. $Z_k^* \cong Z_O^*$).

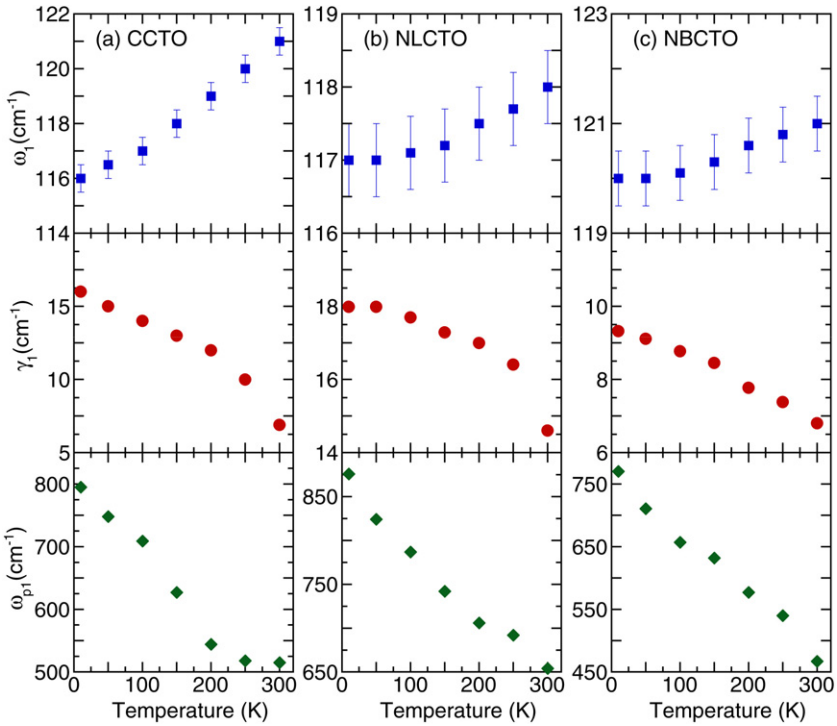

Figure 7. Temperature dependences of frequency, damping and oscillator strength of phonon mode 1 in the (a) CCTO, (b) NLCTO and (c) NBCTO compounds.

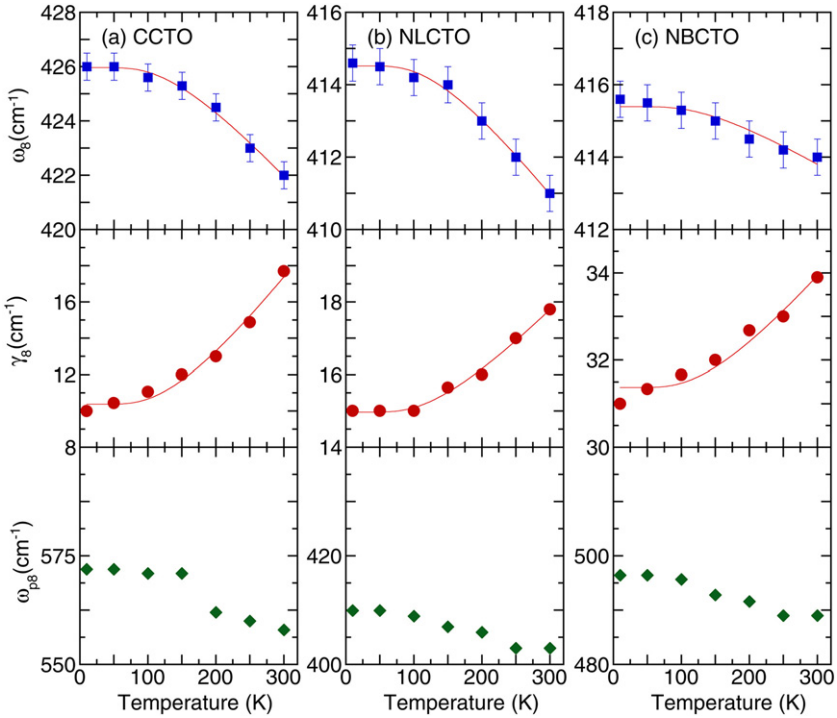

Figure 8. Temperature dependences of frequency, damping and oscillator strength of phonon mode 8 in the (a) CCTO, (b) NLCTO and (c) NBCTO compounds. The thin solid lines are results of the fitting taking into account the temperature-induced anharmonicity.

The deduced values for $|Z^*_O|$ are shown in figure 9. At room temperature, the values of $|Z^*_O|$ in two doping samples (1.25 in NLCTO and 1.12 in NBCTO) are smaller than that of CCTO (1.29) due to the different intrinsic properties in three materials (the different electronegativity—the capacity for a material when in a molecule to attract electrons to itself). The electronegativity on the Pauling scale for Na, La, Bi and Ca is set to be 0.93, 1.10, 2.02 and 1.00, respectively. It can be

Table 3. The room-temperature dielectric constant obtained from the analysis of the far-infrared spectra in different high dielectric constant oxides.

Materials	Single-crystalline CCTO [6]	CdCTO [6]	CCTO	NLCTO	NBCTO
$\epsilon_1(0)$	61	71	60	76	54

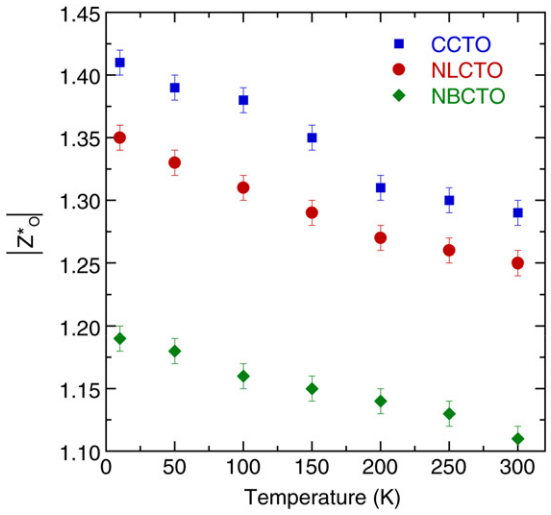

Figure 9. Temperature dependences of the deduced values of Born effective charge per oxygen atom $|Z_O^*|$ in the CCTO, NLCTO and NBCTO compounds.

expected that an atom with higher electron affinity will result in less charge transfer to the oxygen atoms and the reduction in $|Z_O^*|$ is precisely what is, in fact, observed in NLCTO and NBCTO. With decreasing temperature, the increased trend of the $|Z_O^*|$ values is qualitatively consistent with that of spectral weight analysis of the three samples.

The dielectric constant in the far-infrared range can be obtained by fitting the reflectance using a model dielectric function that consists of the sum of several damped oscillators plus a high-frequency permittivity ϵ_∞ originating from the electronic polarization, i.e.

$$\epsilon_1(0) = \sum_j \frac{\omega_{pj}^2}{\omega_j^2} + \epsilon_\infty. \tag{5}$$

Table 3 shows the dielectric constant estimated from the Lorentzian fitting parameters of single-crystalline CCTO [6], ceramic CdCTO [6], CCTO, NLCTO and NBCTO at 300 K. We first notice that the value of $\epsilon_1(0)$ of polycrystalline CCTO is about 60, similar to that of single-crystalline CCTO. Second, NLCTO has a larger dielectric constant than CCTO. It is likely that the vibrational modes of NLCTO are shifted toward lower frequency by 3–10 cm^{-1} with respect to CCTO, resulting in the higher value of $\epsilon_1(0)$ estimated from the equation $(\sum_j \omega_{pj}^2/\omega_j^2)$. Third, the values of the dielectric constant measured by far-infrared spectroscopy for all samples are much smaller than those taken at 100 kHz (∼102 86 in CCTO, 409 in CdCTO, 3560 in NLCTO and 2454 in NBCTO) [2], suggesting an unconventional origin for the giant low-frequency dielectric response observed in these materials. It has been proposed that defects from the IBLC are responsible for this anomalous behavior [9–12]. Such a scenario should be considered to explain why the Na/La or Na/Bi substitution results in a much lower room-temperature value for $\epsilon_1(0)$. But it is unlikely that the twin boundaries in the system acting as the IBLC alone can explain the observed value. Concerns have recently been raised that the large values of $\epsilon_1(0)$ in CCTO are due to considerable substitutional disorder at the Ca/Cu sites [21]. Specifically, the existence of nanoscale disorder of Ca/Cu recovers the orbital degeneracy of Cu, which in turn can induce a metallic-like polarizability in the surrounding insulating regions, hence yielding drastically enhanced dynamical electronic dielectric responses. We can infer that the crucial role of local disorder provides a natural explanation as to why NLCTO and NBCTO have a very different dielectric response from that of CCTO.

4. Summary

In summary, we have studied the structural and optical properties of high dielectric constant NLCTO and NBCTO and compare them with the CCTO compound. Substituting Na/La or Na/Bi for Ca reduces the room-temperature value of the dielectric constant by a factor of 3 to 4. X-ray diffraction data reveal that all Ti–O–Ti angles decrease from a value of 144° for CCTO to 141° for NLCTO and 134° for NBCTO. Such a reduction of Ti–O–Ti angles causes the fairly large tilt of the TiO_6 octahedra, resulting in an increase of the local structural disorder in NLCTO and NBCTO, while at the same time several infrared-active phonon peaks show a broadening in their linewidths for NLCTO and NBCTO, i.e. the coherence in these vibrational modes is degraded by disorder. With decreasing temperature, the lowest-frequency phonon mode is observed to broaden and shift to lower frequency. Moreover, its oscillator strength is found to increase at low temperatures, indicating that the Born effective charges are increasing in the unit cell. Similar behaviors have also been observed in CCTO, but to a lesser extent in NLCTO and NBCTO. The data reported here are helpful in understanding the role of local structural disorder in the unusual dielectric properties of these materials.

Acknowledgments

We would like to gratefully acknowledge financial support from the National Science Council of the Republic of China under grant nos. NSC 95-2112-M-003-021-MY3, 96-2120-M-007-003, 96-2112-M-110-001 and 96-2112-M-032-008-MY3.

References

[1] Subramanian M A, Li D, Duan N, Reisner B A and Sleight A W 2000 *J. Solid State Chem.* **151** 323
[2] Subramanian M A and Sleight A W 2002 *Solid State Sci.* **4** 347

[3] Ramirez A P, Subramanian M A, Gardel M, Blumberg G, Li D, Vogt T and Shapiro S M 2000 *Solid State Commun.* **115** 217
[4] Homes C C, Vogt T, Shapiro S M, Wakimoto S and Ramirez A P 2001 *Science* **293** 673
[5] Kolev N, Bontchev R P, Jacobson A J, Popov V N, Hadjiev V G, Litvinchuk A P and Iliev M N 2002 *Phys. Rev.* B **66** 132102
[6] Homes C C, Vogt T, Shapiro S M, Wakimoto S, Subramanian M A and Ramirez A P 2003 *Phys. Rev.* B **67** 092106
[7] He L, Neaton J B, Cohen M H, Vanderbilt D and Homes C C 2002 *Phys. Rev.* B **65** 214112
[8] He L, Neaton J B, Vanderbilt D and Cohen M H 2003 *Phys. Rev.* B **67** 012013
[9] Sinclair D C, Adams T B, Morrison F D and West A R 2002 *Appl. Phys. Lett.* **80** 2153
[10] Lunkenheimer P, Bobnar V, Pronin A V, Ritus A I, Volkov A A and Loidl A 2002 *Phys. Rev.* B **66** 052105
[11] Liu J J, Duan C G, Yin Wei-Guo, Mei W N, Smith R W and Hardy J R 2004 *Phys. Rev.* B **70** 144106
[12] Chung G Y, Kim I D and Kang S J L 2004 *Nat. Mater.* **3** 774
[13] Kant Ch, Rudolf T, Mayr F, Krohns S, Lunkenheimer P, Ebbinghaus S G and Loidl A 2008 *Phys. Rev.* B **77** 045131
[14] Lunkenheimer P, Fichtl R, Ebbinghaus S G and Loidl A 2004 *Phys. Rev.* B **70** 172102
[15] Krohns S, Lunkenheimer P, Ebbinghaus S G and Loidl A 2007 *Appl. Phys. Lett.* **91** 022910
[16] Larson A C and Von Dreele R B 1994 *Generalized Structure Analysis System, GSAS* (Los Alamos, NM: Los Alamos National Laboratory)
[17] Wooten F 1972 *Optical Properties of Solids* (New York: Academic) p 42
[18] McGuiness C, Downes J E, Sheridan P, Glans P-A, Smith K E, Si W and Johnson P D 2005 *Phys. Rev.* B **71** 195111
[19] Rudolf T, Kant Ch, Mayr F, Hemberger J, Tsurkan V and Loidl A 2007 *Phys. Rev.* B **76** 174307
[20] Scott J L 1971 *Phys. Rev.* B **4** 1360
[21] Zhu Y, Zheng J C, Wu L, Frenkel A I, Hanson J, Northrup P and Ku W 2007 *Phys. Rev. Lett.* **99** 037602